Multifractally-enhanced superconductivity in two-dimensional systems with spin-orbit coupling

E. S. Andriyakhina[1,2] and I. S. Burmistrov[2,3]

[1] *Moscow Institute for Physics and Technology, 141700 Moscow, Russia*
[2] *L. D. Landau Institute for Theoretical Physics, acad. Semenova av. 1-a, 142432 Chernogolovka, Russia*
[3] *Laboratory for Condensed Matter Physics, HSE University, 101000 Moscow, Russia*

The interplay of Anderson localization and electron-electron interactions is known to lead to enhancement of superconductivity due to multifractality of electron wave functions. We develop the theory of multifractally-enhanced superconducting states in two-dimensional systems in the presence of spin-orbit coupling. Using the Finkel'stein nonlinear sigma model, we derive the modified Usadel and gap equations that take into account renormalizations caused by the interplay of disorder and interactions. Multifractal correlations induce energy dependence of the superconducting spectral gap. We determine the superconducting transition temperature and the superconducting spectral gap in the case of Ising and strong spin orbit couplings. In the latter case the energy dependence of superconducting spectral gap is convex whereas in the former case (as well as in the absence of spin-orbit coupling) it is concave. Multifractality enhances not only the transition temperature but, in the same way, the spectral gap at zero temperature. Also we study mesoscopic fluctuations of the local density of states in the superconducting state. Similarly to the case of normal metal, spin-orbit coupling reduce the amplitude of fluctuations.

arXiv:2207.08594v2 [cond-mat.supr-con] 25 Jul 2022

I. INTRODUCTION

Superconductivity and Anderson localization are two fundamental quantum phenomena that have been still attracting great interest. Initially it was believed that non-magnetic disorder does not affect s-wave superconducting order parameter (so-called "Anderson theorem" [1–3]). Later the paradigm was shifted to consider superconductivity and disorder as antagonists due to Anderson localization [4]. Strong localization were predicted to suppress superconductivity [5–8]. Similar destruction of superconductivity was predicted due to Coulomb interaction at weak disorder [9–15]. The experimental discovery [16] of superconductor-to-insulator transition boosted interest to effects of disorder on superconducting correlations in thin films (see Refs. [17–19] for a review).

Recently, the paradigm has been shifted once again. It was predicted in Refs. [20, 21] that Anderson localization can lead to enhancement of the superconducting transition temperature, T_c for systems near the Anderson transition (e.g., in three dimensions). The mechanism is based on the multifractal behavior of wave functions — the well-known companion of Anderson localization — that leads to enhancement of effective attraction between electrons. This mechanism works in the absence of the long-ranged Coulomb repulsion. Later, the multifractal enhancement of T_c has been predicted for systems in the regime of weak localization (or anti-localization) which is relevant for weakly disordered superconducting films [22, 23]. These analytical predictions have been further tested by numerical computations for the disordered attractive Hubbard model on a two-dimensional lattice [24–26]. Recently, a growth of T_c with increase of disorder observed in monolayer niobium dichalcogenides [27, 28] has been suggested as a demonstration of the multifractal-enhancement mechanism.

One way to characterize multifractally-enhanced superconducting state is to study the mesoscopic fluctuations of the local density of states [29, 30]. Potentially, it can be very promising due to (i) many reported tunneling spectroscopy data of the point-to-point fluctuations of the local density of states in thin superconducting films [31–36] and (ii) a qualitative agreement between the theory [37] developed for temperatures $T > T_c$ and experiments on the local density of states in the normal phase of disordered superconducting films.

However, there exist superconducting thin films and two-dimensional systems with broken spin rotational symmetry due to the presence of spin-orbit coupling. Among them one can list single atomic layers of Pb on Si [38], $SrTiO_3$ surfaces [39, 40], $LaAlO_3/SrTiO_3$ interfaces [41, 42], and MoS_2 flakes [43–45]. Moreover, spin orbit coupling of Ising type is expected to exist in monolayer niobium dichalcogenides in which multifractal enhancement of superconductivity was measured [27, 28]. This calls for the theory of multifractally-enhanced superconductivity in two-dimensional systems with spin orbit coupling.

In this work we extend the theory of the multifractal superconducting state developed in Ref. [29] to thin films with spin-orbit coupling. As in Ref. [29] we focus on the case of weak short-ranged electron-electron interaction [1]. We consider an intermediate disorder strength (but still weak) in which analysis of the renormalization group equations for the normal state predicted parametrically enhanced T_c in comparison with the conventional Bardeen-Cooper-Schrieffer (BCS) result [22]. Using the

[1] A long-range component (Coulomb) of interaction can be suppressed in films covered by a substrate with a high dielectric constant.

Finkel'stein nonlinear sigma model, we derive the Usadel equation together with the equation for the spectral gap function. Both equations acquire modifications due to interplay of disorder and interactions at scales shorter than superconducting coherence length. We solve these equations for the cases of Ising-type and strong spin-orbit couplings. In the former case one triplet diffusive mode remains effective at long lengthscales whereas in the latter case all triplet modes are suppressed. In both cases we determine superconducting transition temperature and determine the energy dependence of the spectral gap function at low temperatures, $T \ll T_c$, and in the vicinity of the transition, $T_c - T \ll T_c$. We find that the maximal magnitude of the gap is proportional to T_c, i.e. it is also enhanced by multifractality. In addition, we estimate the mesoscopic fluctuations of the local density of states. We find that these fluctuations are logarithmically divergent with the system size (if one neglects the effect of dephasing) in spite of the absence of spin rotational symmetry.

The outline of the paper is as follows. In Sec. II we present the general scheme for description of the superconducting state. This scheme is applied to the case of Ising-type spin-orbit coupling in Sec. III. In Sec. IV we consider the case of strong spin-orbit coupling. The fluctuations of the local density of states are studied in Sec. V. We end the paper with summary and conclusions in Sec. VI. Some technical details are delegated to Appendices.

II. EQUATION FOR THE SPECTRAL GAP

In dirty superconductors there is substantial energy window between diffusive scale $1/\tau$ (τ stands for the mean free time) and the energy scale related with superconductivity for which one can choose T_c. Therefore, in order to describe superconducting properties which correspond typically to the energy scale T_c (the corresponding length scale is the superconducting coherence length, $\xi = \sqrt{D/T_c}$) one has to take into account effects related with interaction of diffusive modes in the energy interval $T_c \lesssim \varepsilon \lesssim 1/\tau$. As well-known from studies of normal dirty metals, the main effect of diffusive modes is renormalization of physical parameters of the system, e.g. conductance, interaction strengths, etc.

Such renormalization should be taken into account for the superconducting state as well. The most profound effect of the renormalization is the modification of the Usadel equation and the self-consistency equation for the spectral gap. These modified equations can be derived by means of the nonlinear sigma model following approach of Ref. [29] (see details in Appendix A). This procedure results in the following modified Usadel equation for the spectral angle θ_ε,

$$\frac{D_\varepsilon}{2}\nabla^2\theta_\varepsilon - |\varepsilon|\sin\theta_\varepsilon + \Delta_\varepsilon\cos\theta_\varepsilon = 0. \tag{1}$$

Here $\varepsilon = \pi T(2n+1)$ denotes fermionic Matsubara frequency. Equation (1) differs from the standard Usadel equation [46] by energy dependent spectral gap Δ_ε and energy dependent diffusion coefficient D_ε [2].

To the lowest order in disorder and interaction, the spectral gap satisfies the following equation

$$\begin{aligned}\Delta_\varepsilon = &-2\pi T\sum_{\varepsilon'_n>0}\sin\theta_{\varepsilon'}\left\{\gamma_c - 2\frac{(\gamma_s - \mathcal{N}\gamma_t)}{g}\right.\\ &\left.\times\int\frac{d^2\boldsymbol{q}}{(2\pi)^2}\frac{D}{Dq^2 + E_\varepsilon + E_{\varepsilon'}}\right\},\\ E_\varepsilon = &|\varepsilon|\cos\theta_\varepsilon + \Delta\sin\theta_\varepsilon.\end{aligned} \tag{2}$$

Here $\gamma_c < 0$, γ_s, and γ_t stands for the bare values of dimensionless interaction amplitudes in the Cooper channel as well as in the singlet and triplet particle-hole channels, respectively. We assume the interaction in the particle-hole channel to be weak and short-ranged. Therefore, we consider the case of $|\gamma_{c,s,t}| \ll 1$.

The disorder is controlled by the bare dimensionless (in units e^2/h) conductance $g = h/(e^2R_\square)$ where $R_\square$ is the film resistance per square in the normal state. The bare diffusion coefficient D is related with conductance and the density of states, ν, at the Fermi energy in the normal state by means of the Einstein relation $g = 2\pi\nu D$. The superconducting order parameter Δ determines the bare value of the superconducting gap.

Parameter $\mathcal{N}$ in Eq. (2) counts the number of massless triplet diffusive modes. We shall concentrate below on the cases $\mathcal{N} = 0$ and 1 whereas the case $\mathcal{N} = 3$ was considered in Ref. [29].

We note that a similar form of the self-consistency equation for the spectral gap has been derived in Ref. [47, 48] in the case of Coulomb interaction ($\gamma_s = -1$) and neglect of exchange interaction ($\gamma_t = 0$) by means of the diagrammatic technique.

Equation (2) resembles the standard self-consistency equation in the BCS theory except logarithmic renormalization of the attraction interaction parameter γ_c. This renormalization is exactly the same as in the normal metal except the infrared scale is set by $\max\{\varepsilon, \varepsilon', \Delta\}$. The perturbative result (2) for the renormalization of γ_c can be extended by means of the renormalization group technique, see Ref. [29] for details.

Then solving the modified Usadel equation (1) as $\sin\theta_\varepsilon = \Delta_\varepsilon/\sqrt{\varepsilon^2 + \Delta_\varepsilon^2}$, we find the following self-consistency relation for Δ_ε:

$$\Delta_\varepsilon = -2\pi T\sum_{\varepsilon'>0}\frac{\gamma_c\left(L_{E_\varepsilon+E_{\varepsilon'}}\right)\Delta_{\varepsilon'}}{\sqrt{\varepsilon'^2 + \Delta_{\varepsilon'}^2}}, \tag{3}$$

[2] In this paper we are interested in the superconducting state which is spatially homogeneous on the scale of the order of ξ. Therefore, we shall not discuss energy dependence of the diffusion coefficient here.

Here $L_\varepsilon = \sqrt{D/\varepsilon}$ is the diffusive length associated with the energy scale ε. The flow of γ_c with the length scale L is governed by the following renormalization group equation (see Ref. [29] for $\mathcal{N} = 3$),

$$\frac{d\gamma_c}{dy} = -\frac{t}{2}(\gamma_s - \mathcal{N}\gamma_t). \tag{4}$$

Here $y = \ln L/\ell$ with ℓ and L being the mean free path and the system size, respectively. The dimensionless resistance is denoted as $t = 2/(\pi g)$. Its bare value t_0 is assumed to be small, $t_0 \ll 1$.

Equation (4) does not contain the standard term, -γ_c^2, which is responsible for the Cooper instability in the clean case. This term is encoded in the superconducting order parameter Δ (see Ref. [29] for details).

It is tempting to substitute Δ by Δ_ε in the expression for E_ε in Eq. (3) to make it fully self-consistent equation for Δ_ε. This is exactly what was done in Ref. [29] based on the relation between the Usadel equation linearized in variation of θ_ε and the Cooperon propagator with coinciding energies. However, further analysis demonstrates that Cooperon propagator with two non-equal Matsubare energies has more complicated structure after renormalization. [3] Fortunately, as we shall see below the precise form of difference $E_\varepsilon - |\varepsilon|$ is not essential for results reported in this paper.

Eq. (4) is needed to be supplemented by renormalization group equations for $\gamma_{s,t}$ and t. However, their precise form depends on the magnitude of $\mathcal{N}$. Below we shall analyse Eq. (3) separately for the cases $\mathcal{N} = 0$ and 1. In what follows we assume that bare values of interaction and disorder are weak: $|\gamma_{s0}|, |\gamma_{t0}|, |\gamma_{c0}|, t_0 \ll 1$.

III. $\mathcal{N} = 1$: ISING SPIN-ORBIT COUPLING

In this section we focus on superconducting films with the so-called Ising spin orbit coupling. The latter pins electron spins to the out-of-plane direction. In this case in-plane spin-flip scattering rates, induced by spin-orbit coupling are smaller than the out-of-plane one, $1/\tau_{\rm so}^{x,y} \ll 1/\tau_{\rm so}^{z}$. Hence, one triplet diffusive mode, corresponding to the total spin projection $S_z = 0$, remains gapless as well as singlet diffusive mode. That is why the case $\mathcal{N} = 1$ is realized for the Ising spin-orbit coupling.

In order to analyse the gap equation (3) one needs to know the actual dependence of γ_c on the length scale. In Ref. [23] the full set of one-loop renormalization group equations for $\gamma_{s,t,c}$ and t has been derived by means of the background field renormalization of the nonlinear sigma model above superconducting transition temperature. Applying the same method in the superconducting state, we find

$$\frac{dt}{dy} = -\frac{t^2}{2}(\gamma_s + \gamma_t + 2\gamma_c), \tag{5a}$$

$$\frac{d}{dy}\begin{pmatrix}\gamma_s\\ \gamma_t\\ \gamma_c\end{pmatrix} = -\frac{t}{2}\begin{pmatrix}1 & 1 & 2\\ 1 & 1 & -2\\ 1 & -1 & 0\end{pmatrix}\begin{pmatrix}\gamma_s\\ \gamma_t\\ \gamma_c\end{pmatrix}. \tag{5b}$$

We note that Eq. (5a) is written under assumption that $|\gamma_{s,t,c}| \ll 1$. In the same way as in the normal metal [49], weak localization and weak antilocalization compensate each other in the presence of Ising spin-orbit coupling. Eq. (5a) implies that dimensionless resistance t remains almost constant in the leading order. Therefore, we shall assume $t \simeq t_0$ below. Equation (5b) suggests that under the renormalization group flow the interaction parameters approach the so-called the BCS line $-\gamma_s = \gamma_t = \gamma_c \equiv \gamma$ [22]. In order to describe the behavior of the system at lengthscales $y \gtrsim t_0^{-1}$, we project Eq. (5b) onto the BCS line. Then we shall work with effective interaction parameter γ that flows according to

$$d\gamma/dy \simeq t_0\gamma, \quad \gamma_0 = (\gamma_{t0} - \gamma_{s0} + 2\gamma_{c0})/4 < 0. \tag{6}$$

Solving the above equation, we find

$$\gamma(L) = \gamma_0(L/\ell)^{t_0}. \tag{7}$$

Below we assume that disorder dominates interaction, i.e. $t_0 \gg |\gamma_0|$. As known [22], it is the regime in which the multifracal enhancement of superconducting transition temperature is expected. The transition temperature T_c can be estimated from the relation $|\gamma(L_{T_c})| \sim t_0$ (see Appendix B). It yields

$$T_c \sim (1/\tau)(|\gamma_0|/t_0)^{2/t_0}. \tag{8}$$

We note that the superconducting critical temperature T_c corresponds to $y_c \sim t_0^{-1}\ln(t_0/|\gamma_0|) \gg t_0^{-1}$. This justifies the projection onto the BCS line.

A. The critical temperature

More accurately the superconducting transition temperature T_c can be determined from the linearized self-consistent equation, cf. Eq. (3). We note that after projection of the self-consistency equation (3) onto the BCS line, γ_c in it is substituted by γ. Linearized version of the self-consistency equation then reads

$$\Delta_\varepsilon = -2\pi T\sum_{\varepsilon'>0}\gamma(L_{\varepsilon+\varepsilon'})\frac{\Delta_{\varepsilon'}}{\varepsilon'}. \tag{9}$$

Taking into account the actual dependence of $\gamma(L)$ on L, Eq. (7), we find

$$\Delta_n = \frac{|\gamma_0|}{(2\pi T\tau)^{t_0/2}}\sum_{n'\geqslant 0}^{n_{\max}}\frac{\Delta_{n'}}{(n+n'+1)^{t_0/2}(n'+1/2)}, \tag{10}$$

[3] The authors are grateful to P. Nosov for this comment.

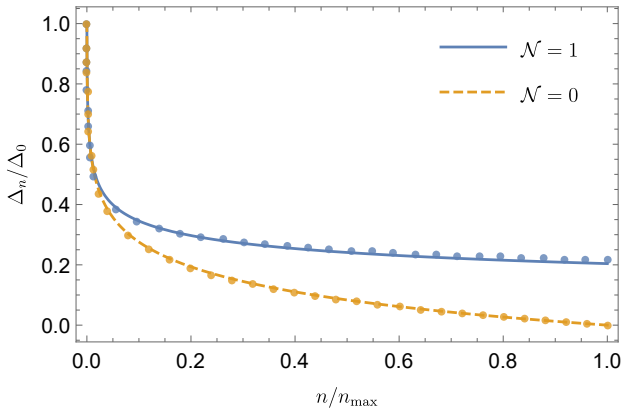


FIG. 1. The dependence of the gap function Δ_n on the Matsubara energies $\varepsilon_n = 2\pi T(n+1/2)$ for T near the critical temperature T_c. Solid and dashed lines show analytical expressions (15) and (41), respectively. Dots of the corresponding colors mark numerical solutions for leading eigenvectors of Eqs. (10) and (36).

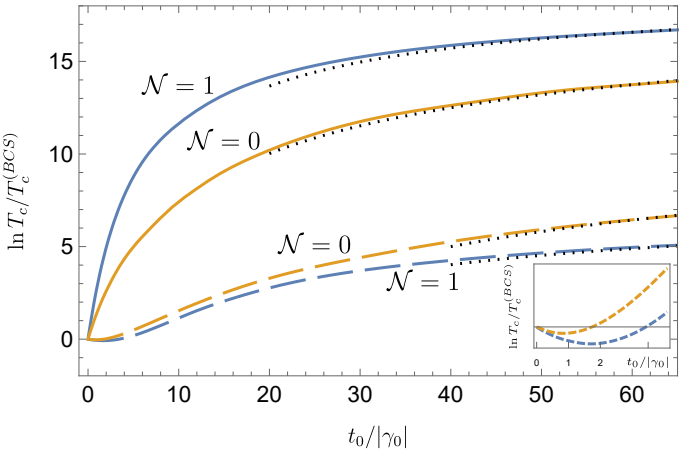


FIG. 2. Multifractally-increased superconducting transition temperature T_c. Solid lines show the dependence of $\ln T_c/T_c^{(BCS)}$ on magnitude of the ratio $t_0/|\gamma_0|$, when the initial interaction parameters γ_{s0}, γ_{t0}, γ_{c0} lie on the BCS-line, i.e. $-\gamma_s = \gamma_t = \gamma_c = \gamma$ for $\mathcal{N}=1$ and $-\gamma_s = \gamma_c = \gamma$ for $\mathcal{N}=0$. Dashed lines of the corresponding colors illustrate the behavior of $\ln T_c/T_c^{(BCS)}$, when the initial parameters deviate from the BCS-line. This can lead to a decrease in the critical temperature T_c in comparison to $T_c^{(BCS)}$ at a small ratio of t_0 to $|\gamma_0|$ (see inset), but eventually $\ln T_c/T_c^{(BCS)}$ becomes positive and continues to grow with increasing disorder. Black dotted lines correspond to expressions (16) and (42).

where $n_{\max} \simeq 1/(2\pi T\tau)$ is the natural cut off for number of Matsubara frequencies belonging to the diffusive regime. The search for T_c in Eq. (10) can be reformulated as a problem of the maximal eigenvalue of the corresponding matrix. The superconducting transition temperature satisfies $(2\pi T_c\tau)^{t_0/2} = |\gamma_0|\lambda_M$ where λ_M is the maximal eigenvalue of the matrix $M_{nn'} = (n+n'+1)^{-t_0/2}(n'+1/2)^{-1}$.

Numerical solution of Eq. (10) by the means of the power method (see Appendix C) gives $\lambda_M \simeq 1.4/t_0$ such that

$$T_c \simeq \frac{1}{2\pi\tau}(1.4|\gamma_0|/t_0)^{2/t_0}. \tag{11}$$

The right eigenvector r_n of the matrix M corresponding to λ_M is shown in Fig. 1. (The left eigenvector of the matrix M is expressed as $l_n = r_n/(n+1/2)$.) There is a significant energy dependence of the spectral gap in contrast with the BCS model for which it is just a constant.

The result (11) can be also justified on the basis of analytical treatment of Eq. (10). Let us first replace $(n+n'+1)^{t_0/2}$ with $\max\{(n+1/2)^{t_0/2}, (n'+1/2)^{t_0/2}\}$. It is justified by the smallness of exponent $t_0 \ll 1$. Next we introduce a variable

$$u_\varepsilon = \frac{2}{t_0}|\gamma(L_\varepsilon)| = \frac{2|\gamma_0|}{t_0}(\varepsilon\tau)^{-t_0/2}. \tag{12}$$

Then, employing the Euler-Maclaurin resummation to the right hand side of Eq. (9), we obtain

$$\Delta_{u_n} \simeq u_n\int_{u_n}^{u_0} du\frac{\Delta_u}{u} + \int_{u_\infty}^{u_n} du\Delta_u + \frac{at_0}{2}u_n\Delta_{u_0}, \tag{13a}$$

$$u_\infty \equiv u_{1/\tau} \sim |\gamma_0|/t_0 \ll 1, \tag{13b}$$

$$a = 1 + \sum_{k=1}^{\infty} 2^{2k-1}B_{2k}/k \approx 1.27. \tag{13c}$$

Here u_∞ corresponds to $n_{\max}$ and B_{2k} denotes even Bernoulli numbers. At $T = T_c$ we seek the solution of Eq. (13a) in the form $\Delta_{u_n} = \Delta_{u_0}f(u_n)$ with the normalization $f(u_0) = 1$. The integral equation (13a) can be reduced to the following Cauchy problem for the unknown function $f(u)$,

$$f''(u) = -f(u)/u,$$
$$f'(u_0) = at_0/2, \qquad f'(u_\infty) = f(u_\infty)/u_\infty. \tag{14}$$

Solving Eq. (14), we obtain

$$f(u) = \frac{F_1(u)}{F_1(u_0)}, \quad F_1(u) \simeq \sqrt{u}J_1(2\sqrt{u}). \tag{15}$$

Here $J_1(x)$ denotes the Bessel function of the first kind. We note that for the sake of brevity in the above expression $F_1(u)$ is written in the lowest order in small parameters $|\gamma_0| \ll t_0 \ll 1$. Although one can easily find the exact solution to $f(u)$, in what follows we do not need it.

We also note that the solution (15) satisfies the normalization condition $f(u_0) = 1$ and the boundary condition at $u = u_\infty$. The yet unknown parameter u_0 determines the superconducting transition temperature as

$$T_c = (2\pi\tau)^{-1}((2/u_0)|\gamma_0|/t_0)^{2/t_0}. \tag{16}$$

It can be extracted from the boundary condition at $u = u_0$. Using the relation $(xJ_1(x))' = xJ_0(x)$ and neglecting $at_0/2$ in the right hand side of the equation for the boundary condition at $u = u_0$, we find $u_0 \simeq (j_{0,1})^2/4 \approx 1.45$ where $j_{n,k}$ is the k-th zero of the Bessel $J_n(x)$ function. The result (16) is in quantitative agreement with the result (11) of numerical approach. Moreover, as shown in Fig. 1, there is a remarkable agreement between the function $f(u_n)$ and numerically computed eigenvector corresponding to the maximal eigenvalue of the matrix M.

Equation (11) predicts increase of T_c with increase of disorder, t_0, at fixed γ_0. However, Eq. (11) is valid for $t_0 \gg |\gamma_0|$ only. We solve the self-consistency equation (10) for various t_0 numerically. The obtained dependence of T_c on t_0 is shown in Fig. 2. As one can see, for initial conditions at the BCS line T_c grows with increase of t_0 reaching the asymptotic expression (16) (black dotted lines) at $t_0 \gg |\gamma_0|$. In case of the system away from the BCS line initially, at first, T_c is suppressed with increase of t_0, but then it starts to grow at $t_0 \gtrsim |\gamma_0|$.

We now move on to examining the behaviour of the gap function Δ_ε as a function of ε at different temperature regimes: when T is close to T_c and when $T \ll T_c$.

B. The spectral gap function

1. *The gap function near T_c*

At $T = T_c$ the amplitude Δ_0 of the spectral gap function vanishes. To find the dependence of Δ_ε on energy at $T_c - T \ll T_c$, we expand the modified self-consistency equation to the third order, retrieving

$$\Delta_\varepsilon = 2\pi T \sum_{\varepsilon'>0} |\gamma(L_{\varepsilon+\varepsilon'})| \left(\frac{\Delta_{\varepsilon'}}{\varepsilon'} - \frac{\Delta^3_{\varepsilon'}}{2\varepsilon'^3} \right). \tag{17}$$

We note that quadratic in Δ_ε terms that originate from expansion of $\left|\gamma(L_{E_\varepsilon+E_{\varepsilon'}})\right|$ are suppressed by a small factor $t_0 \ll 1$.

Let us write $\Delta_{\varepsilon_n} = \Delta_0(T) r_n$ with the normalization $r_0 = 1$. Then Eq. (17) becomes

$$\lambda_M \left(\frac{T}{T_c}\right)^{\frac{t_0}{2}} r_n = \sum_{n'=0}^{n_{\max}} M_{nn'} \left[r_{n'} - \frac{\frac{\Delta_0^2(T)}{8\pi^2 T_c^2} r^3_{n'}}{(n'+1/2)^2} \right]. \tag{18}$$

In order $\Delta_0(T_c) = 0$, one need to choose r_n to be the right eigenvector of the matrix $M_{nn'}$, corresponding to its maximal eigenvalue λ_M. Then, multiplying both sides of Eq. (18) on the left eigenvector $l_n = r_n/(n+1/2)$ (corresponding to λ_M) from the left, we find

$$\Delta_0(T) = \left(b_{\mathcal{N}} \frac{8\pi^2}{7\zeta(3)} T_c(T_c - T) \right)^{1/2}. \tag{19}$$

Here the constant $b_{\mathcal{N}}$ for $\mathcal{N} = 1$ is given as

$$b_1 = \frac{7\zeta(3)t_0}{2} \frac{\sum\limits_{n=0}^{n_{\max}} r_n^2/(n+1/2)}{\sum\limits_{n=0}^{n_{\max}} r_n^4/(n+1/2)^3}. \tag{20}$$

We chose normalization of b_1 in such a way that the quantity $b_1 - 1$ describes the deviation from the BCS theory. Although, one could expect the nonzero value for the difference $b_1 - 1$ due to strong energy dependence of the right eigenvector, as we shall demonstrate below, this is not the case within our approximation.

First of all, replacing r_n^4 with $r_0^4 = 1$ in the denominator of Eq. (20), we find that

$$\sum_{n=0}^{n_{\max}} \frac{r_n^4}{(n+1/2)^3} \simeq 7\zeta(3). \tag{21}$$

Next, in order to estimate the numerator of Eq. (20), we replace r_n with an analytical expression $r_n = f(u_n)$, see Eq. (15). Hence, we obtain

$$\sum_{n=0}^{n_{\max}} \frac{r_n^2}{n+1/2} \simeq \frac{2}{t_0} \int_0^{u_0} \frac{du}{u} f^2(u) \simeq \frac{2}{t_0}. \tag{22}$$

Combining all the above we restore the BCS results, $b_1 = 1$, in the limit $t_0 \ll 1$. We note that in order to compute corrections to the BSC result, $b_1 = 1$, one needs to know the precise form of dependence of the infrared cut off length scale $L_{E_\varepsilon+E_{\varepsilon'}}$ on Δ_ε and $\Delta_{\varepsilon'}$ in Eq. (3).

One can estimate the effect of admixture of other eigenmodes to the dependence of Δ_ε on ε. Writing $\Delta_\varepsilon = \Delta_0(T)(r_n + \sum_j s_j r_n^{(j)})$ where $r_n^{(j)}$ are the right eigenvectors of the matrix M with eigenvalues $\lambda_j < \lambda_M$, we find

$$s_j = -\frac{\lambda_j}{\lambda_M - \lambda_j} \frac{\Delta_0^2(T)}{8\pi^2 T_c^2} \frac{\sum\limits_{n=0}^{N} l_n^{(j)} r_n^3/(n+1/2)^2}{\sum\limits_{n=0}^{N} l_n^{(j)} r_n^{(j)}}. \tag{23}$$

Here we used orthogonality condition $\sum_n l_n^{(j)} r_n = 0$ where $l_n^{(j)}$ stands for the left eigenvector of the matrix $M_{nn'}$ corresponding to the eigenvalue λ_j. We see that the admixture of the other eigenmodes at $T_c - T \ll T_c$ is completely negligible. Therefore, the energy dependence of Δ_ε on ε at $T_c - T \ll T_c$ is essentially the same as at the transition.

2. The gap function at $T \ll T_c$

We start from the zero-temperature limit. To study the behaviour of the gap function at $T = 0$ we substitute summation over Matsubara frequencies by integration over energy ε' in Eq. (3). We note that there are two sources for dependence on ε'. The fast dependence under the square root and slow (almost logarithmic for $t_0 \ll 1$) dependence in γ. On the basis of the solution for $T = T_c$ we expect Δ_ε to be decreasing function of ε. Let us introduce the characteristic energy scale ε_0, such that $\Delta_{\varepsilon_0} = \varepsilon_0$. The structure of the equation on Δ_ε, see Eq. (3), suggests that the gap-function slightly varies from its value Δ_0 at $\varepsilon = 0$ to $\Delta_{\varepsilon_0} = \varepsilon_0$ at $\varepsilon = \varepsilon_0$. This implies that $\varepsilon_0 \sim \Delta_0$. In order to find the precise relation between ε_0 and Δ_0 as well as dependence of Δ_ε at $\varepsilon < \Delta_0$, one needs to know the precise dependence of the infrared length scale $L_{E_\varepsilon + E_{\varepsilon'}}$ on Δ_ε and $\Delta_{\varepsilon'}$, see Eq. (3). This complication is absent at large energies $\varepsilon \gg \Delta_\varepsilon$. As we shall check below, the latter condition is fulfilled at energies ε not too close to Δ_0, i.e. at $\varepsilon \gtrsim \Delta_0$, due to the smallness of dimensional resistance, $t_0 \ll 1$.

At $\varepsilon \gg \Delta_\varepsilon$ we approximate the self-consistent equation (3) as follows

$$\Delta_\varepsilon \simeq |\gamma(L_\varepsilon)| \int\limits_0^{\Delta_0} \frac{d\varepsilon' \Delta_0}{\sqrt{\varepsilon'^2 + \Delta_0^2}} + |\gamma(L_\varepsilon)| \int\limits_{\Delta_0}^{\varepsilon} \frac{d\varepsilon' \Delta_{\varepsilon'}}{\sqrt{\varepsilon'^2 + \Delta_{\varepsilon'}^2}} + \int\limits_{\varepsilon}^{1/\tau} \frac{d\varepsilon' \Delta_{\varepsilon'}}{\sqrt{\varepsilon'^2 + \Delta_{\varepsilon'}^2}} |\gamma(L_{\varepsilon'})|. \tag{24}$$

Substituting Δ_ε for $\Delta_{u_\varepsilon} = \Delta_{u_0} f(u_\varepsilon)$, where u_ε is defined in Eq. (12), the above equation can be rewritten in the following differential form

$$f''(u_\varepsilon) = -\frac{\varepsilon f(u_\varepsilon)/u_\varepsilon}{\sqrt{\varepsilon^2 + \Delta_0^2 f^2(u_\varepsilon)}}. \tag{25}$$

Since we are working in the regime $\varepsilon \gg \Delta_\varepsilon$, we can safely neglect the term with Δ_0 under the square root in the right hand side of Eq. (25). Then Eq. (25) reduces to Eq. (14) with the same boundary conditions except $a = \operatorname{arcsinh}(1)$ now. Thus the solution can be read from Eq. (15). Altogether we find the following solution for the spectral gap function

$$\Delta_\varepsilon \simeq \Delta_0 \begin{cases} 1, & \varepsilon \lesssim \Delta_0, \\ F_1(u_\varepsilon)/F_1(u_{\Delta_0}), & \varepsilon \gtrsim \Delta_0. \end{cases} \tag{26}$$

Now we can check the assumption $\varepsilon \gg \Delta_\varepsilon$. Using Eq. (26), we find that

$$\frac{\varepsilon}{\Delta_\varepsilon} = \frac{u_{\Delta_0}^{2/t_0} F_1(u_{\Delta_0})}{u_\varepsilon^{2/t_0} F_1(u_\varepsilon)} \gg 1 \tag{27}$$

holds for all ε except close vicinity of $|\varepsilon - \Delta_0| \sim \Delta_0$.

We note perfect matching of both asymptotic results (26) at $\varepsilon = \Delta_0$. Using the boundary condition $f'(u_{\Delta_0}) = 0$ we find that Δ_0 coincides with T_c upto numerical prefactor,

$$\Delta_0 \sim T_c. \tag{28}$$

However, as we noted above our approach does not applicable in the vicinity of the point $\varepsilon = \Delta_0$. Therefore, we cannot determine the precise constant for the ratio for Δ_0/T_c. We emphasize that the dependence of the spectral gap function at $\varepsilon \gg \Delta_0$ for $T = 0$ is exactly the same as for T close to T_c.

We emphasize that the spectral gap function is parametrically enhanced at small energies. Using Eq. (26) we find that the spectral gap at $\varepsilon \sim 1/\tau$ (which coincides with the order parameter Δ) is proportional to $\Delta_0 |\gamma_0|/t_0 \ll \Delta_0$. Typical behaviour of Δ_ε is illustrated in Fig. 3.

At non-zero temperature, the form of the spectral gap function remains the same but there is reduction of the magnitude of Δ_0 while temperature increases. At $T \ll \Delta_0$ the dependence of Δ_0 on temperature can be estimated as follows. At $\varepsilon \gg \Delta_0$ the gap function Δ_ε satisfies equation similar to Eq. (24) in which Δ_0 is substituted by $\Delta_0(T)$ and

$$\int\limits_0^{\Delta_0} \frac{d\varepsilon' \Delta_0}{\sqrt{\varepsilon'^2 + \Delta_0^2}} \to 2\pi T \sum_{\varepsilon' > 0} \frac{\Delta_0(T)}{\sqrt{\varepsilon'^2 + \Delta_0^2(T)}} - \int\limits_{\Delta_0(T)}^{1/\tau} \frac{d\varepsilon' \Delta_0(T)}{\sqrt{\varepsilon'^2 + \Delta_0^2(T)}} \simeq \int\limits_0^{\Delta_0(T)} \frac{d\varepsilon' \Delta_0(T)}{\sqrt{\varepsilon'^2 + \Delta_0^2(T)}} - \sqrt{\frac{2\pi T}{\Delta_0}} e^{-\Delta_0/T}. \tag{29}$$

Such modification of Eq. (24) results in change of the constant a in the boundary conditions in Eq. (14). Now it becomes $a = \operatorname{arcsinh}(1) - \sqrt{2\pi T/\Delta_0} \exp(-\Delta_0/T)$. Taking this temperature shift of the constant a into account, we find

$$\Delta_0 - \Delta_0(T) \sim \sqrt{2\pi T \Delta_0}\, e^{-\Delta_0/T}, \quad T \ll \Delta_0. \tag{30}$$

We note that since this result is obtained with the help of the boundary condition at $\varepsilon = \Delta_0(T)$, we cannot unambiguously determine a numerical factor in Eq. (30).

IV. $\mathcal{N} = 0$: STRONG SPIN-ORBIT COUPLING

In this section we consider the case when all three spin-flip rates, $1/\tau_{\rm so}^{x,y,z}$, induced by the spin-orbit coupling are of the same order. Then diffusive modes corresponding to the total spin zero remain gapless only. Thus the number of triplet modes reduces to zero, $\mathcal{N} = 0$.

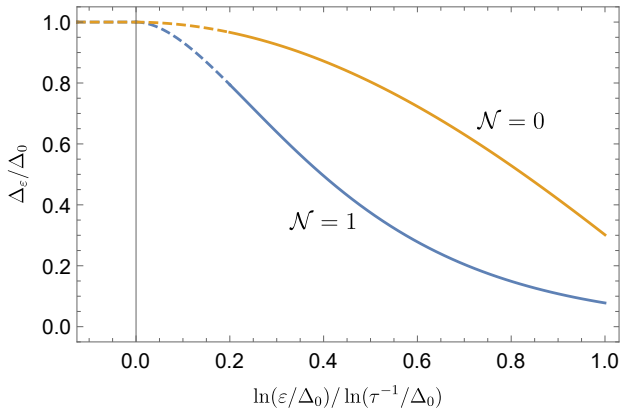


FIG. 3. The dependence of the gap function Δ_ε at low temperatures on energy ε (see text). Dimensionless interaction constant is chosen to be $|\gamma_0| = 0.005$ and dimensionless resistance is $t_0 = 0.2$. Bottom curve illustrates the behaviour of Δ_ε for the case of Ising spin-orbit coupling ($\mathcal{N} = 1$) while the top one corresponds to the case of strong spin-orbit coupling ($\mathcal{N} = 0$).

For $\mathcal{N} = 0$ the renormalization group flow of the interaction parameters $\gamma_{s,c}$ and the dimensionless resistance t is governed by the following equations [23]

$$\frac{dt}{dy} = -t^2(1+\gamma_s+2\gamma_c)/2, \tag{31a}$$

$$\frac{d}{dy}\begin{pmatrix}\gamma_s\\ \gamma_c\end{pmatrix} = -\frac{t}{2}\begin{pmatrix}1 & 2\\ 1 & 0\end{pmatrix}\begin{pmatrix}\gamma_s\\ \gamma_c\end{pmatrix}. \tag{31b}$$

We emphasize that contrary to the case $\mathcal{N} = 1$ there is the weak-antilocalization correction (term with unity in the brackets in the right hand side of Eq. (31a)) that results in flow of t towards zero. In what follows we neglect terms proportional to $\gamma_{s,c}$ (Altshuler-Aronov and density-of-states-type corrections) in Eq. (31a) in comparison with weak antilocalization. In accordance with Eq. (31b), the interaction parameters flow approaching the BCS line $-\gamma_s = \gamma_c \equiv \gamma$. Projecting Eq. (31b) onto the BCS line, we find

$$d\gamma/dy = t\gamma/2, \quad \gamma_0 = (2\gamma_{c0} - \gamma_{s0})/3 < 0. \tag{32}$$

Here γ_0 is the initial value of the effective attraction. We assume $t_0 \gg |\gamma_0|$. Solving Eqs. (31a) and (32), we obtain

$$t(L) = \frac{t_0}{1+(t_0/2)\ln L/\ell}, \qquad \gamma(L) = \gamma_0\frac{t_0}{t(L)}. \tag{33}$$

The effective attraction is growing with increase of the length scale. The superconducting critical temperature can be estimated from the condition $|\gamma(L_{T_c})| \sim t(L_{T_c})$ (see Appendix B). It results in the estimate [22]

$$\ln 1/(T_c\tau) \sim \frac{1}{\sqrt{|\gamma_0|t_0}}. \tag{34}$$

We note that the numerical factor cannot be determined reliably in this way.

A. The critical temperature

Let us now, in order to determine the superconducting transition temperature, solve the self-consistent equation (9). It is convenient to introduce parametrization of the critical temperature in the form

$$T_c = (2\pi\tau)^{-1}\exp\left(4/t_0 - 4/t_c\right), \tag{35}$$

where, based on Eq. (34), we expect t_c to be of the order of $\sqrt{|\gamma_0|t_0}$. Hence Eq. (9) becomes

$$\Delta_n = \frac{|\gamma_0|t_0}{4}\sum_{n'=0}^{n_{\max}}\frac{4/t_c - \ln(n+n'+1)}{n'+1/2}\Delta_{n'}. \tag{36}$$

Here $n_{\max} = 1/(2\pi T_c\tau) \simeq \exp(4/t_c)$. Again Eq. (36) can be considered as the maximal eigenvalue problem for the matrix $M_{nn'}(\zeta) = (\zeta - \ln(n+n'+1))/(n'+1/2)$ with $\zeta = 4/t_c$. Numerical solution for the maximal eigenvalue reveals $\lambda_M \approx 0.41(4/t_c)^2$ (see Appendix C). Thus we find

$$t_c \approx 1.3\sqrt{|\gamma_0|t_0}. \tag{37}$$

The dependence of the right eigenvector corresponding to the maximal eigenvalue found numerically is shown in Fig. 1.

Similar to the case $\mathcal{N} = 1$, we are able to solve the linearized self-consistency equation (9) analytically. Introducing the variable

$$u_\varepsilon = \frac{4}{t(L_\varepsilon)} = \frac{4|\gamma(L_\varepsilon)|}{|\gamma_0|t_0} = \frac{4}{t_0} - \ln(\varepsilon\tau), \tag{38}$$

replacing $\ln(n+n'+1)$ with $\ln(\max\{n+1/2, n'+1/2\})$, and using the Euler-Maclaurin formula, we get

$$\frac{4\Delta_{u_n}}{|\gamma_0|t_0} = u_n\int_{u_n}^{u_0} du\Delta_u + \int_{u_\infty}^{u_n} duu\Delta_u + au_n\Delta_{u_0}. \tag{39}$$

Here a coincides with the one defined in Eq. (13c). Next, writing $\Delta_{u_n} = \Delta_{u_0}f(u_n)$ with $f(u_0) = 1$, we cast the above equation in the following differential equation,

$$f''(u) = -(|\gamma_0|t_0/4)f(u),$$
$$f(u_0) = 1, \quad f'(u_\infty) = \frac{f(u_\infty)}{u_\infty}, \quad f'(u_0) = \frac{|\gamma_0|t_0}{4}. \tag{40}$$

The latter can be elementary solved:

$$f(u) = \frac{F_0(u)}{F_0(u_0)}, \quad F_0(u) \simeq \sin\left[u\sqrt{|\gamma_0|t_0/4}\right] \tag{41}$$

Again, in the above equation the solution to $f(u)$ is written in the lowest order in the small parameters $|\gamma_0| \ll t_0 \ll 1$. The last step is to find $u_0 = 4/t_c$ from the relation $f'(u_0) = |\gamma_0|t_0/4$. Simple algebra yields

$$u_0 \simeq \pi/\sqrt{|\gamma_0|t_0}, \quad \Leftrightarrow \quad t_c \simeq \frac{4}{\pi}\sqrt{|\gamma_0|t_0}. \tag{42}$$

We point out remarkable agreement between the numerical and the analytical results, Eq. (37) and Eq. (42): 1.3 and $4/\pi$, respectively.

The numerical solution of Eq. (36) for T_c with arbitrary values of t_0 is shown in Fig. 2. Analytical expression (42) (marked with a black dotted line) gives correct asymptotic values of $\ln T_c/T_c^{(BCS)}$ in the regime of large ratio $t_0/|\gamma_0|$.

B. The spectral gap function

1. The gap function near T_c

At temperatures $T_c - T \ll T_c$ we use Eq. (17) in order to find Δ_ε. We parametrize the temperature T by t_T, such that $T = (2\pi\tau)^{-1}\exp(4/t_0 - 4/t_T)$. After one writes $\Delta_\varepsilon = \Delta_0(T)r_n$, Eq. (17) becomes

$$\lambda_M r_n \simeq \sum_{n'=0}^{n_{\max}} M_{nn'}(4/t_T)\left[r_{n'} - \frac{\frac{\Delta_0^2(T)}{8\pi^2T_c^2}r_{n'}^3}{(n'+1/2)^2}\right], \quad (43)$$

Here, we remind, λ_M denotes the maximal eigenvalue of the matrix $M_{nn'}(4/t_c)$. Using the identity $M_{nn'}(4/t_T) = M_{nn'}(4/t_c) + (4/t_T - 4/t_c)/(n'+1/2)$ and approximation $4/t_T - 4/t_c \approx (T_c - T)/T_c$, we rewrite Eq. (43) as

$$\lambda_M(4/t_c)r_n \simeq \sum_{n'=0}^{n_{\max}} M_{nn'}(4/t_c)\left[r_{n'} - \frac{\frac{\Delta_0^2(T)}{8\pi^2T_c^2}r_{n'}^3}{(n'+1/2)^2}\right] + \frac{T_c - T}{T_c}\sum_{n'=0}^{n_{\max}}\frac{r_{n'}}{n'+1/2}. \quad (44)$$

When $T = T_c$ the gap function turns to zero. This implies that r_n are the components of the leading eigenvector of matrix $M_{nn'}(4/t_c)$. Multiplying Eq. (44) on the left eigenvector of $M_{nn'}(4/t_c)$, $l_n = r_n/(n+1/2)$, we retrieve the result (19) with $b_\mathcal{N}$ for $\mathcal{N} = 0$ being

$$b_0 = \frac{7\zeta(3)}{\lambda_M}\frac{\left(\sum\limits_n^{n_{\max}} r_n/(n+1/2)\right)^2}{\sum\limits_{n=0}^{n_{\max}} r_n^4/(n+1/2)^3}. \quad (45)$$

As in the case of $\mathcal{N} = 1$ one can check that within our approximation $b_0 = 1$ as in the BCS theory. The denominator in the right hand side of Eq. (45) is treated in the same fashion as in the case of $\mathcal{N} = 1$. While in the numerator we write $r_n = f(u_n)$, where $f(u)$ is given in Eq. (41). Using $F_0(u) = \sin(u/\sqrt{\lambda_M})$ and $u_0 = \sqrt{\lambda_M}\pi/2$, one immediately finds

$$\left(\sum_{n=0}^{n_{\max}}\frac{r_n}{n+1/2}\right)^2 \simeq \left(\int_0^{u_0} du\, f(u)\right)^2 = \lambda_M. \quad (46)$$

Therefore, combining the results for numerator and denominator we restore $b_0 = 1$.

2. The gap function at $T \ll T_c$

The spectral gap function at $T = 0$ can be found in the same way as it was done in Sec. III B 2 for $\mathcal{N} = 1$. After straightforward calculations, we find

$$\Delta_\varepsilon \simeq \Delta_0\begin{cases}1, & \varepsilon \lesssim \Delta_0,\\ F_0(u_\varepsilon)/F_0(u_{\Delta_0}), & \varepsilon \gtrsim \Delta_0.\end{cases} \quad (47)$$

The maximal magnitude of the spectral gap, Δ_0, is given by the expression similar to Eq. (35),

$$\Delta_0 = (2\pi\tau)^{-1}e^{4/t_0 - 4/t_{\Delta_0}}, \quad t_{\Delta_0} \sim \sqrt{|\gamma_0|t_0}. \quad (48)$$

Unfortunately, within our approximation we cannot unambiguously determine the numerical factor in the ratio $t_{\Delta_0}/\sqrt{|\gamma_0|t_0}$ since it requires knowledge of the precise dependence of the infrared lengthscale $L_{E_\varepsilon + E_{\varepsilon'}}$ on Δ_ε and $\Delta_{\varepsilon'}$, see Eq. (3). Since t_{Δ_0} stands in the exponent of the expression for Δ_0, we cannot exclude a possibility that Δ_0 differs parametrically from T_c.

We note that the superconducting order parameter (which coincides with the spectral gap function at energies $\varepsilon \sim 1/\tau$) is proportional to $\Delta_0\sqrt{|\gamma_0|/t_0} \ll \Delta_0$. Typical dependence of Δ_ε on ε is shown in Fig. 3.

The change of Δ_ε with increasing temperature is the same as in the case of $\mathcal{N} = 1$. At $T \ll T_c$ the amplitude Δ_0 is decreasing in accordance with Eq. (30).

V. LOCAL DENSITY OF STATES

In this section we discuss the local density of states and its mesoscopic fluctuations in the superconducting state. For the sake of simplicity we consider $T = 0$.

The disorder-averaged density of states can be found from the solution of the Usadel equation

$$\langle\rho(E)\rangle = \nu\Re\cos\theta_{\varepsilon\to -iE+0} = \nu\Re\frac{\varepsilon}{\sqrt{\varepsilon^2+\Delta_\varepsilon^2}}\Big|_{\varepsilon\to -iE+0}. \quad (49)$$

Here the analytical continuation from Matsubara energies to real energies is performed, $i\varepsilon \to E + i0$.

The behavior of the density of states at energies E close to Δ_0 depends on fine structure of Δ_ε at $\varepsilon \sim \Delta_0$. Thus we have no access to these range of energies. The only statement is possible to make is the existence of the spectral gap of the order of Δ_0. Away from Δ_0, i.e. at $E \gtrsim \Delta_0$, using the smallness of $\Delta_\varepsilon/\varepsilon$, we find

$$\frac{\langle\rho(E)\rangle}{\nu} \simeq 1 + \Re\frac{\Delta^2(E)}{2E^2} \simeq 1 + \frac{\Delta_0^2}{2E^2}\frac{F_\mathcal{N}^2(u_E)}{F_\mathcal{N}^2(u_{\Delta_0})}. \quad (50)$$

Here $u_E = u_{\Delta_0}(E/\Delta_0)^{-t_0/2}$ and $u_E = u_{\Delta_0} - \ln(E/\Delta_0)$ for $\mathcal{N} = 1$ and 0, respectivelty.

Now we estimate mesoscopic fluctuations of the local density of states. This can be done using the nonlinear

sigma model approach in a way similar to the one of Ref. [29]. We restrict our consideration by energy range

$$\Delta_0 \ll \frac{1}{\tau} e^{-2(2-\mathcal{N})/t_0} \ll E \lesssim \frac{1}{\tau}. \tag{51}$$

In this range we can neglect the energy dependence of Δ_ε and approximate it by its non-renormalized value Δ. Then we obtain for the variance of the local density of states the following result (see Appendix D)

$$\frac{\langle[\delta\rho(E,\boldsymbol{r})]^2\rangle}{\nu^2} = \frac{1+\mathcal{N}}{g}\,\mathrm{Re}\int \frac{d^2\boldsymbol{q}}{(2\pi)^2}\left[\frac{2E^2-\Delta^2}{E^2-\Delta^2}\frac{1}{q^2} + \frac{\Delta^2}{E^2-\Delta^2}\frac{D}{Dq^2+2i\sqrt{E^2-\Delta^2}}\right]. \tag{52}$$

We note that the contribution in the first line of Eq. (52) corresponds to correlations between electron-like and electron-like excitations. They do not feel the superconducting spectral gap. This explains why the infrared divergence in diffusive propagator persist inside superconductor. The contribution in the second line of Eq. (52) is due to correlations between electron-like and hole-like excitations which are split by the twice the superconducting gap.

Performing integration over momentum and expansion in $\Delta/E \ll 1$, we find

$$\frac{\langle[\delta\rho(E,\boldsymbol{r})]^2\rangle}{\langle\rho(E)\rangle^2} = \frac{(1+\mathcal{N})t_0}{2}\Big(\ln\frac{L}{\ell} + \frac{\Delta^2}{2E^2}\ln\frac{L_E}{\ell}\Big). \tag{53}$$

We emphasize logarithmic divergence of the variance with the system size L. This signals about strong mesoscopic fluctuations of the local density of states in disordered superconductors with the spin-orbit coupling similar to the case when the spin-orbit coupling is absent [29, 30].

The renormalization of diffusive propagator ignored so far results in substitution of L by $\min\{L, L_E^{(\phi)}\}$ where $L_E^{(\phi)}$ denotes the dephasing length induced by electron-electron interactions. Unfortunately, at present, there is no complete theory of dephasing rate in disordered superconductors. Using the results of Ref. [50], one can estimate dephasing length due to electron-electron interaction at $E \gg \Delta$ as $L_\Delta/(|\gamma_0|\sqrt{t_0}) \gg L_\Delta$. We note that such estimate is applicable at $T \ll T_c$. Close to superconducting transition the dephasing rate is enhanced due to the superconducting fluctuations (for details see Ref. [51]).

With the help of the renormalization group we can convert the perturbative, infrared divergent, result (53) into the result for the second moment of the local density of state:

$$\frac{\langle\rho^2(E,\boldsymbol{r})\rangle}{\langle\rho(E)\rangle^2} = \begin{cases} (\min\{L, L_E^{(\phi)}\}/\ell)^{t_0}, & \mathcal{N}=1, \\ 1+(t_0/2)\ln(\min\{L, L_E^{(\phi)}\}/\ell), & \mathcal{N}=0. \end{cases} \tag{54}$$

One can also generalize expression (53) to the pair correlation function of the local density of states at differing energies $E \gg \Delta$ and $E' = E+\omega \gg \Delta$ (see Appendix D),

$$\frac{\langle\delta\rho(E,\boldsymbol{r})\delta\rho(E',\boldsymbol{r})\rangle}{\langle\rho(E)\rangle\langle\rho(E')\rangle} \simeq \frac{(1+\mathcal{N})t_0}{2}\ln\frac{\min\{L, L_E^{(\phi)}, L_\omega\}}{\ell}. \tag{55}$$

For the autocorrelation function of moments one can use Eq. (54) in which $\min\{L, L_E^{(\phi)}\}$ should be substituted by $\min\{L, L_E^{(\phi)}, L_\omega\}$.

We note that one can compute the disorder-averaged higher moments of the local density of states. Similarly to the case without spin-orbit interaction [29], the moments correspond to the log-normal distribution for the local density of states.

VI. SUMMARY AND CONCLUSIONS

To summarize, we have developed the theory of the multifractally-enhanced superconducting state in thin films with spin-orbit coupling under assumption of the presence of weak short-ranged electron-electron interaction. We considered the case of Ising spin-orbit coupling ($\mathcal{N}=1$) for which renormalization of the normal state resistance is negligible and the case of strong spin-orbit coupling ($\mathcal{N}=0$) in which renormalization of t is dominated by weak-antilocalization correction. Together with the case without spin-orbit coupling ($\mathcal{N}=3$) studied in Ref. [29], we have now the theory for all three possible behavior of the normal state resistance with the system size: increasing, decreasing and constant.

Following approach of Ref. [29], we treated the fluctuations around the mean-field spatially homogeneous saddle-point and derived the modified Usadel equation and self-consistency equation that incorporates the interplay of disorder and interactions at high energies. The derived equations allows us to determine accurately the superconducting transition temperature. The later is enhanced (even for ($\mathcal{N}=0$) in comparison with the BCS result in the absence of disorder. The solution of the modified Usadel equation and self-consistency equation yields T_c which coincides parametrically with the estimate from the Cooper-channel instability in renormalization group equations for the normal phase. It is worth comparing the multifractally increased critical temperatures for different number of triplet modes. In the absence of spin-orbit coupling, see Ref. [29], superconducting phase is expected to be present for temperatures lower than $T_c^{\mathcal{N}=3} \sim \tau^{-1}\exp(-2/t_0)$. In contrast, we predict $T_c^{\mathcal{N}=1} \sim \tau^{-1}\exp(-(2/t_0)\ln(t_0/(1.4|\gamma_0|)))$ for $\mathcal{N}=1$ and $T_c^{\mathcal{N}=0} \sim \tau^{-1}\exp(-3.1/\sqrt{|\gamma_0|t_0})$ for $\mathcal{N}=0$, respectively. Therefore, T_c increases with the number of triplet diffusive modes: $T_c^{\mathcal{N}=3} \gg T_c^{\mathcal{N}=1} \gg T_c^{\mathcal{N}=0}$.

The disorder-induced energy dependence of the effective attraction translates into the energy dependence of

the spectral gap function. The form of this energy dependence is sensitive to the number of triplet modes $\mathcal{N}$. In the case $\mathcal{N}=1$ the energy dependence of the spectral gap is concave (the same holds for $\mathcal{N}=3$), see Fig. 3. For $\mathcal{N}=0$ Δ_ε becomes convex function of ε. The interplay of disorder and interactions lead to parametrical enhancement of the spectral gap function at low energies in comparison with its magnitude at energies $\sim 1/\tau$.

In spite of such strong distinction from the BCS theory in which the spectral gap function is independent of the energy, the basic relations for the BCS model: behavior of the gap just below T_c and at low temperatures $T \ll T_c$, remain untouched. This indicates that one can use the BCS theory in order to describe the temperature dependence of the spectral gap in weakly disordered films. In the presence of spin-orbit coupling we revealed strong mesoscopic fluctuations of the local density of states in the superconducting state. These fluctuations persist upto the lengthscale set by the dephasing length. The presence of spin-orbit coupling reduces the amplitude of the variance of the local density of states by a factor 2 (for $\mathcal{N}=1$) and by a factor 4 (for $\mathcal{N}=0$). Due to different energy dependence of the gap function for different $\mathcal{N}$, the energy dependence of the variance is sensitive to the number of massless triplet modes. The most pronounced difference is expected near the coherence peak, $E \sim \pm\Delta_0$. However this region is beyond the accuracy of our calculations.

It is instructive to compare the fluctuations of the local density of states with the fluctuations of the superconducting order parameter. We note that although our approach assumes spatially constant order parameter one can study its mesoscopic fluctuations. In the case of the presence of the spin-orbit coupling, we find

$$\frac{\langle(\delta\Delta)^2\rangle}{\Delta^2} \simeq \frac{(1+\mathcal{N})t_0}{2}\ln\frac{L_{\Delta_0}}{\ell}. \tag{56}$$

We emphasize the close similarity between Eq. (55) and (56). However, there is a crucial difference: the mesoscopic fluctuations of the superconducting order parameter are controlled by the coherence length L_{Δ_0} in the infrared. Since $L_E^{(\phi)} \gg L_{\Delta_0}$ we expect $\langle(\delta\rho)^2\rangle/\langle\rho\rangle^2 \gg \langle(\delta\Delta)^2\rangle/\Delta^2$. For $\mathcal{N}=1$ ($\mathcal{N}=0$) we can estimate $\langle(\delta\Delta)^2\rangle/\Delta^2$ as $\sim \ln(t_0/|\gamma_0|)$ ($\sim \sqrt{t_0/|\gamma_0|}$), respectively.

The results presented in this paper can be generalized in several directions. Most interesting to study renormalization of the diffusive propagators and to formulate the equation for the spectral gap in a fully self-consistent way. With such equation in hands one can determine Δ_0 upto the numerical factor in order to compare it with the expression for T_c. Also such computation for the diffusive propagators allows to determine the dephasing length serving a cut-off for the mesoscopic fluctuations of the local density of states. Further our theory can be extended to include the Coulomb interaction. Additionally, it would be interesting to go beyond weak-coupling for superconductivity and to study the multifractal effects at the BCS – BEC crossover [52, 53]. Also our work can be extended to consider systems with singular dynamical interaction between electrons, see Refs. [54–59], in the presence of disorder. This can be achieved along the approaches of Refs. [60, 61].

Finally, we mention that our theory ignores phase fluctuations of the order parameter. The latter are known to be responsible for the Berezinskii- Kosterlitz-Thouless transition in superconducting films. Such fluctuations can be taken into account in the way similar to the one in Refs. [62, 63]. However, for weakly disordered superconducting films effects related with phase fluctuations are expected to be weak [62, 64].

Authors are grateful to C. Brun, T. Cren, F. Evers, I. Gornyi, M. Lizee, A. Mirlin, P. Nosov, S. Raghu, and M. Stosiek for collaboration on related projects and useful discussions. The research is partially supported by the Russian Foundation for Basic Research (Grant No. 20-52- 12013) and by the Basic Research Program of HSE.

Appendix A: Finkel'stein nonlinear sigma model

In this Appendix we present details of the Finkel'stein nonlinear sigma model formalism.

The action of an electron liquid in a disordered metal with spin-orbit coupling is given by

$$S = S_\sigma + S_{\rm int}^{(\rho)} + S_{\rm int}^{(\sigma)} + S_{\rm int}^{(c)} + S_{\rm so}, \tag{A1}$$

where the first term comes from non-interacting fermions. The next three terms correspond to electron-electron interactions in the particle-hole singlet channel, $S_{\rm int}^{(\rho)}$, in the particle-hole triplet channel, $S_{\rm int}^{(\sigma)}$, and in the particle-particle channel $S_{\rm int}^{(c)}$. The last term appears due to spin-orbit coupling. The above mentioned contributions reads (see Refs. [67–69] for review)

$$S_\sigma = -\frac{g}{32}\int_{\boldsymbol{r}} \mathrm{Tr}(\nabla Q)^2 + 2Z_\omega \int_{\boldsymbol{r}} \mathrm{Tr}\,\hat{\varepsilon}Q \tag{A2a}$$

$$S_{\rm int}^{(\rho)} = -\frac{\pi T}{4}\Gamma_s \sum_{r=0,3}\sum_{\alpha,n}\int_{\boldsymbol{r}} \mathrm{Tr}\, I_n^\alpha t_{r0} Q\, \mathrm{Tr}\, I_{-n}^\alpha t_{r0} Q \tag{A2b}$$

$$S_{\rm int}^{(\sigma)} = -\frac{\pi T}{4}\Gamma_t \sum_{\substack{r=0,3\\ j=1,2,3}}\sum_{\alpha,n}\int_{\boldsymbol{r}} \mathrm{Tr}\, I_n^\alpha t_{rj} Q\, \mathrm{Tr}\, I_{-n}^\alpha t_{rj} Q \tag{A2c}$$

$$S_{\rm int}^{(c)} = -\frac{\pi T}{4}\Gamma_c \sum_{r=1,2}\sum_{\alpha,n}\int_{\boldsymbol{r}} \mathrm{Tr}\, t_{r0} L_n^\alpha Q\, \mathrm{Tr}\, t_{r0} L_n^\alpha Q \tag{A2d}$$

$$S_{\rm so} = \frac{\pi\nu}{2}\sum_{j=1,2,3}\frac{1}{\tau_{\rm so}^{(j)}}\int_{\boldsymbol{r}} \mathrm{Tr}(t_{0j}Q)^2 \tag{A2e}$$

In what is written above g is the total Drude conductivity (in units e^2/h and including spin). The parameter Z_ω describes the renormalization of the frequency term [67]. Its bare value is given as $\pi\nu/4$. Interaction amplitudes in the singlet, the triplet, and the particle-hole

channels are designated as Γ_s, Γ_t, and Γ_c, respectively. It is convenient to introduce the dimensionless interaction parameters $\gamma_{s,t,c} \equiv \Gamma_{s,t,c}/Z_\omega$. $1/\tau_{\rm so}^{(j)}$ stands for the spin-orbit scattering rates.

The matrix field $Q(\boldsymbol{r})$ and the trace Tr operate in the replica (α,β), Matsubara (n,m), spin $(j=0,1,2,3)$, and particle-hole $(r=0,1,2,3)$ spaces. The matrix field $Q(\boldsymbol{r})$ obeys the nonlinear constraint, as well as the charge-conjugation symmetry relation

$$Q^2=1, \quad \mathrm{Tr}\, Q=0, \quad Q=Q^\dagger=-CQ^TC, \tag{A3}$$

where $C=it_{12}$ and the matrix t_{rj} is

$$t_{rj}=\tau_r\otimes s_j, \quad r,j=0,1,2,3. \tag{A4}$$

In the expression above r and j subscripts correspond to particle-hole and spin spaces, respectively. τ_r and s_j denote standard Pauli matrices,

$$\begin{aligned} \tau_0/s_0&=\begin{pmatrix}1&0\\0&1\end{pmatrix}, \quad \tau_1/s_1=\begin{pmatrix}0&1\\1&0\end{pmatrix},\\ \tau_2/s_2&=\begin{pmatrix}0&-i\\i&0\end{pmatrix}, \quad \tau_3/s_3=\begin{pmatrix}1&0\\0&-1\end{pmatrix}. \end{aligned} \tag{A5}$$

Taking constraints (A3) into account, we use the following parametrization for the matrix field $Q(\boldsymbol{r})$

$$\begin{aligned} Q=U^{-1}\Lambda U, \quad U^\dagger=U^{-1}, \quad CU^T=U^{-1}C,\\ \Lambda^{\alpha\beta}_{nm}=\mathrm{sgn}\,\varepsilon_n\delta_{\varepsilon_n,\varepsilon_m}\delta^{\alpha\beta}t_{00} \end{aligned} \tag{A6}$$

The constant matrices in the action (A1) are given by the following expressions ($\omega_k=2\pi Tk$):

$$\begin{aligned} \hat{\varepsilon}^{\alpha\beta}_{nm}&=\varepsilon_n\delta_{\varepsilon_n,\varepsilon_m}\delta^{\alpha\beta}t_{00},\\ (I^\gamma_k)^{\alpha\beta}_{nm}&=\delta_{\varepsilon_n-\varepsilon_m,\omega_k}\delta^{\alpha\beta}\delta^{\alpha\gamma}t_{00},\\ (L^\gamma_k)^{\alpha\beta}_{nm}&=\delta_{\varepsilon_n+\varepsilon_m,\omega_k}\delta^{\alpha\beta}\delta^{\alpha\gamma}t_{00}. \end{aligned} \tag{A7}$$

Following Ref. [29], we employ the above technique to describe the low-energy physics in the broken symmetry superconducting state. In order to do so one needs to single out the static term with $n=0$ in the particle-particle channel, see Eq. (A2d), and introduce two decoupling fields $\Delta^\alpha_r(\boldsymbol{r})$ with $r=1,2$. Upon Hubbard–Stratonovich transformation one finds

$$\begin{aligned} S^{(c)}_{\rm int}=\sum_{r=1,2}\int_{\boldsymbol{r}}\Bigg[&\frac{4Z_\omega}{\pi T\gamma_c}[\Delta^\alpha_r(\boldsymbol{r})]^2+2Z_\omega\Delta^\alpha_r(\boldsymbol{r})\,\mathrm{Tr}\,t_{r0}L^\alpha_0Q\\ &-\frac{\pi T}{4}\Gamma_c\sum_{n\neq0}\left(\mathrm{Tr}\,t_{r0}L^\alpha_nQ\right)^2\Bigg]. \end{aligned} \tag{A8}$$

Variation of the total action with respect to $Q(\boldsymbol{r})$ and $\Delta^\alpha_r(\boldsymbol{r})$ give rise to the Usadel equation and the self-consistency relations for $\Delta^\alpha_r(\boldsymbol{r})$, $r=1,2$. In turn, these equations may generate many spatially dependent solutions. In order to account for them we assume $1/g\ll1$ and exploit the renormalization group technique by treating the spatially dependent solutions $Q(\boldsymbol{r})$ as fluctuations around some spatially independent solution $\underline{Q}$.

This program can be performed as follows. At first, we distinguish spatially independent and spatially dependent components of the fields $\Delta^\alpha_r(\boldsymbol{r})$, $r=1,2$, they read

$$\Delta^\alpha_r(\boldsymbol{r})=\underline{\Delta}^\alpha_r+\delta\Delta^\alpha_r(\boldsymbol{r}), \quad \int_{\boldsymbol{r}}\delta\Delta^\alpha_r(\boldsymbol{r})=0. \tag{A9}$$

We point out that fluctuations of the order parameter are now contained in $\delta\Delta^\alpha_r(\boldsymbol{r})$. On the other hand, one can perform a formally exact integration over the fields $\delta\Delta^\alpha_r(\boldsymbol{r})$ in the action. The latter transfers information about fluctuations of the order parameter entirely onto the field $Q(\boldsymbol{r})$. Accordingly, we get

$$\begin{aligned} S^{(c)}_{\rm int}=2Z_\omega V\sum_\alpha\sum_{r=1,2}\left\{\underline{\Delta}^\alpha_r\,\mathrm{Tr}\,t_{r0}L^\alpha_0\overline{Q}+\frac{2}{\pi T\gamma_c}\left[\underline{\Delta}^\alpha_r\right]^2\right\}\\ +\hat{S}^{(c)}_{\rm int}, \end{aligned} \tag{A10}$$

where V is the volume of a superconductor,

$$\overline{Q}=\frac{1}{V}\int_{\boldsymbol{r}}Q(\boldsymbol{r}), \tag{A11}$$

and

$$\hat{S}^{(c)}_{\rm int}=-\frac{\pi T}{4}\Gamma_c\sum_{\alpha,n}\sum_{r=1,2}\int_{\boldsymbol{r}}\left(\mathrm{Tr}\,t_{r0}L^\alpha_nQ_n\right)^2. \tag{A12}$$

Where $Q_n=Q-\overline{Q}\delta_{n,0}$.

The described above procedure leads to a new saddle-point equation for $Q(\boldsymbol{r})$ and self-consistency equations for $\underline{\Delta}^\alpha_r$,

$$\begin{aligned} &D\nabla(Q\nabla Q)-[\hat{\varepsilon}+\hat{\underline{\Delta}},Q]+\frac{\pi T}{4}\sum_{\alpha,n}\Bigg[\sum_{r=1,2}\gamma_c[t_{r0}L^\alpha_n,Q]\\ &\times\mathrm{Tr}\,t_{r0}L^\alpha_nQ_n+\sum_{r=0,3}\sum_{j=0}^{3}\gamma_j[I^\alpha_{-n}t_{rj},Q]\,\mathrm{Tr}\,I^\alpha_nt_{rj}Q\Bigg]=0,\\ &\underline{\Delta}^\alpha_r=\frac{\pi T}{4}|\gamma_c|\,\mathrm{Tr}\,t_{r0}L^\alpha_0\overline{Q}, \quad r=1,2\,. \end{aligned} \tag{A13}$$

Now, one can investigate solutions of the latter equations. In the mean-field description one ignores fluctuations, seeking a spatially independent solution solely. This solution can be conveniently parametrized with the so-called spectral angle, θ_{ε_n}, which is function of Matsubara energies ε_n. In terms of the spectral angle the saddle-point solution reads

$$\begin{aligned} \underline{Q}=R^{-1}\Lambda R, \qquad R^{\alpha\beta}_{nm}=\Big[&\delta_{\varepsilon_n,\varepsilon_m}\cos\frac{\theta_{\varepsilon_n}}{2},\\ &-t_\phi\delta_{\varepsilon_n,-\varepsilon_m}\,\mathrm{sgn}\,\varepsilon_m\sin\frac{\theta_{\varepsilon_n}}{2}\Big]\delta^{\alpha\beta}\\ t_\phi=\cos\phi\;t_{10}+\sin\phi\;t_{20},&\\ \underline{\Delta}^\alpha_1=\Delta\cos\phi, \qquad \underline{\Delta}^\alpha_2=\Delta\sin\phi.& \end{aligned} \tag{A14}$$

Substituting the expressions for $\underline{Q}$ and $\underline{\Delta}_r^\alpha$ from (A14) into the Usadel and self-consistent equations, we find

$$\frac{D}{2}\nabla^2\theta_{\varepsilon_n} - |\varepsilon_n|\sin\theta_{\varepsilon_n} + \Delta\cos\theta_{\varepsilon_n} = 0, \tag{A15a}$$

$$\Delta = \pi T|\gamma_c|\sum_{\varepsilon_n}\sin\theta_{\varepsilon_n}. \tag{A15b}$$

The spatially independent solution of Eq. (A15a) reduces Eq. (A15b) to the usual self-consistent equation of the BCS theory. Thus T_c becomes insensitive to disorder in accordance with the "Anderson theorem".

However, we are interested in more intricate picture, when fluctuations of $Q(\boldsymbol{r})$ around the saddle-point solution $\underline{Q}$ are taken into consideration. The latter corresponds to the interaction of the diffusive modes. We use the square-root parametrization of the matrix field to get the perturbative expansion of $Q(\boldsymbol{r})$ field around the saddle-point solution,

$$Q = R^{-1}\Big(W + \Lambda\sqrt{1-W^2}\Big)R, \quad W = \begin{pmatrix} 0 & w \\ \overline{w} & 0 \end{pmatrix}. \tag{A16}$$

Here W-field satisfies the charge-conjugation constraints:

$$\overline{w} = -Cw^TC, \qquad w = -Cw^*C. \tag{A17}$$

Before moving on to fluctuations, we also need to know the propagators for diffusive modes. We limit ourselves to the lowest order in residual electron-electron interactions, which corresponds to small magnitudes of the bare interaction parameters $|\gamma_{s0,t0,c0}| \ll 1$. Within this approximation, one finds

$$\Big\langle [w_{rj}(\boldsymbol{p})]^{\alpha_1\beta_1}_{n_1n_2}[\overline{w}_{rj}(-\boldsymbol{p})]^{\beta_2\alpha_2}_{n_4n_3}\Big\rangle = \frac{2}{g}\delta^{\alpha_1\alpha_2}\delta^{\beta_1\beta_2}\delta_{\varepsilon_{n_1},\varepsilon_{n_3}} \times\delta_{\varepsilon_{n_2},\varepsilon_{n_4}}\mathcal{D}_p(i\varepsilon_{n_1}, i\varepsilon_{n_2}),$$

$$\mathcal{D}_p(i\varepsilon_{n_1}, i\varepsilon_{n_2}) = \frac{1}{p^2 + E_{\varepsilon_{n_1}}/D + E_{\varepsilon_{n_2}}/D}, \tag{A18}$$

where we remind $E_{\varepsilon_n} = |\varepsilon_n|\cos\theta_{\varepsilon_n} + \Delta\sin\theta_{\varepsilon_n}$. It is crucial to keep in mind here that the result (A18) ignores spin-orbit term in the action, $S_{\rm so}$. It leads to appearance of additional mass term (proportional to $1/\tau_{\rm so}$) in the denominator of the diffusive propagators (A18). Thus the corresponding modes will be suppressed in the diffusive limit. In other words, in the above equations j accounts only for the gapless modes, i.e. $j = 0$ for $\mathcal{N} = 0$ and $j = 0, 3$ for $\mathcal{N} = 1$.

Hereby we are all set to investigate how the fluctuations of Q renormalizes the NLSM action. To the lowest order in disorder we approximate Q as $Q \simeq \underline{Q} + R^{-1}WR$. This yields the following fluctuation correction from the interacting part of the action (in the particle-hole channel),

$$S^{(\rho)}_{\rm int} + S^{(\sigma)}_{\rm int} \to -\frac{\pi T}{4}\int_{\boldsymbol{r}}\sum_{\alpha,n}\sum_{r=0,3}\sum_j \Gamma_j\langle {\rm Tr}\big[RI^\alpha_n t_{rj}R^{-1}W\big] \times {\rm Tr}\big[RI^\alpha_{-n}t_{rj}R^{-1}W\big]\rangle. \tag{A19}$$

Here and later a summation is performed over $j = 0$ for $\mathcal{N} = 0$ and over $j = 0, 3$ for $\mathcal{N} = 1$. Given the expression for the propagators (A18), we obtain (for more details see Ref. [29])

$$S^{(\rho)}_{\rm int} + S^{(\sigma)}_{\rm int} \to \frac{32\pi TN_rV}{g}(\Gamma_s - \mathcal{N}\Gamma_t) \times\sum_{\varepsilon,\varepsilon'>0}\sin\theta_\varepsilon\sin\theta_{\varepsilon'}\int_q \mathcal{D}_q(i\varepsilon, -i\varepsilon')\ , \tag{A20}$$

where $\int_q \equiv \int d^2\boldsymbol{q}/(2\pi)^2$. In its turn, the interaction in the Cooper channel renormalizes as follows

$$\hat{S}^{(c)}_{\rm int} \to -\frac{32\pi T\Gamma_cN_r}{g}\sum_{\varepsilon>0}\mathcal{D}_{q=0}(i\varepsilon, -i\varepsilon)\sin^2\theta_\varepsilon. \tag{A21}$$

Together Eqs. (A20) and (A21) contribute to the following modified action

$$S[\underline{Q}] \to 16\pi TZ_\omega N_rV\Bigg\{\frac{\Delta^2}{4\pi T\gamma_c} + \sum_{\varepsilon>0}\Big[\varepsilon\cos\theta_\varepsilon + \Delta\sin\theta_\varepsilon\Big] + \frac{2\pi T(\gamma_s - \mathcal{N}\gamma_t)}{g}\sum_{\varepsilon,\varepsilon'>0}\sin\theta_\varepsilon\sin\theta_{\varepsilon'}\int_q\mathcal{D}_q(i\varepsilon, -i\varepsilon')\Bigg\}. \tag{A22}$$

Finally, variation of Eq. (A22) with respect to θ_ε and Δ, leads to Eqs. (1) and (2), accordingly.

Appendix B: Critical temperature

In this appendix we estimate the critical temperature using the renormalization group equations describing the renormalization of resistivity and interactions in the normal phase. The full set of one-loop (lowest order in disorder) renormalization group equations has been derived by means of the background field renormalization of the Finkelstein nonlinear sigma model, see Eqs. (47)-(51) in Ref. [23]. Expanding these equations in $|\gamma_{s,t,c}| \ll 1$ and choosing $\mathcal{N} = 1$, we find

$$\frac{dt}{dy} = -t^2(\gamma_s + \gamma_t + 2\gamma_c])/2, \tag{B1a}$$

$$\frac{d}{dy}\begin{pmatrix}\gamma_s\\ \gamma_t\\ \gamma_c\end{pmatrix} = -\frac{t}{2}\begin{pmatrix}1 & 1 & 2\\ 1 & 1 & -2\\ 1 & -1 & 0\end{pmatrix}\begin{pmatrix}\gamma_s\\ \gamma_t\\ \gamma_c\end{pmatrix} - \begin{pmatrix}0\\ 0\\ 2\gamma_c^2\end{pmatrix}. \tag{B1b}$$

Equation (B1a) implies that dimensionless resistance t remains constant and equals to its bare value t_0. Projecting Eqs. (B1b) onto the BCS line $-\gamma_s = \gamma_t = \gamma_c = \gamma$ we obtain

$$\frac{d\gamma}{dy} = t_0\gamma - \gamma^2, \quad \gamma_0 = (\gamma_{t0} - \gamma_{s0} + 2\gamma_{c0})/4 < 0. \tag{B2}$$

After solving the equation written above, we find that renormalization group flow diverges at $y_c = t_0^{-1}\ln(1 +$

$t_0/|\gamma_0|$). When $|\gamma_0| \ll t_0 \ll 1$ it yields considerable enhancement of superconductivity, $T_c \sim (1/\tau)e^{-2y_c}$, cf. Eq. (8). We note that for $|\gamma_0| \ll t_0 \ll 1$ the attraction interaction γ reaches value t_0 at the lengthscale $y_c - \ln 2$ and, then, very rapidly diverges.

Next we tackle the case $\mathcal{N} = 0$ in the same manner. Strong spin-orbit coupling fully suppresses all triplet modes and equations for the remaining interactions γ_s, γ_c along with resistivity t read

$$\frac{dt}{dy} = -t^2/2, \tag{B3a}$$

$$\frac{d}{dy}\begin{pmatrix}\gamma_s\\ \gamma_c\end{pmatrix} = -\frac{t}{2}\begin{pmatrix}1 & 2\\ 1 & 0\end{pmatrix}\begin{pmatrix}\gamma_s\\ \gamma_c\end{pmatrix} - \begin{pmatrix}0\\ 2\gamma_c^2\end{pmatrix}. \tag{B3b}$$

Projection of the latter system onto the BCS line $-\gamma_s = \gamma_c = \gamma$ gives

$$\frac{d\gamma}{dy} = (t/2)\gamma - (4/3)\gamma^2, \quad \gamma_0 = (2\gamma_{c0} - \gamma_{s0})/3 < 0. \tag{B4}$$

Similarly to the case discussed above, in the regime $|\gamma_0| \ll t_0 \ll 1$ $|\gamma|$ grows with increase of y and reaches t. After this happen, $|\gamma|$ very quickly diverges at the length-scale $y_c \sim 1/\sqrt{|\gamma_0|t_0}$. The latter corresponds to the following critical temperature $T_c \sim (1/\tau)e^{-2y_c}$, cf. Eq. (34) .

Appendix C: Numerical solution

In the current appendix we provide some details of the numerical solution for the critical temperature. For this purpose power iteration and dimensional fitting are employed.

As mentioned in the main text, linearized self-consistency equation Eq. (9) can be thought of as an eigenvalue problem. However, the difficulty from a numerical point of view lies in the fact that the matrices defined in Eqs. (10) and (36) are parametrically large. Indeed, $n_{\max} \simeq 1/2\pi\tau T_c$ yields $n_{\max} \propto (t_0/|\gamma_0|)^{2/t_0} \gg 1$ for $\mathcal{N} = 1$ and $n_{\max} \propto \exp(4/t_c - 4/t_0) \gg 1$ for $\mathcal{N} = 0$. Below we treat both cases separately.

When Ising spin-orbit coupling is considered, we fit the leading eigenvector with the expression

$$\lambda_M = c_1/t_0 + c_2, \tag{C1}$$

where c_1 and c_2 are the fitting parameters. This formula is justified by the following analytical estimate,

$$\lambda_M = \sum_{n'\geqslant 0}^{n_{\max}} \frac{\Delta_{n'}/\Delta_0}{(n'+1)^{t_0/2}(n'+1/2)} \simeq \frac{2}{t_0}\int_{u_\infty}^{u_0}\frac{du}{u_0}f(u) + c_2 = c_1/t_0 + c_2. \tag{C2}$$

This reveals the functional dependence of the leading eigenvalue λ_M on the parameter $t_0 \ll 1$. In the above expression we have used the asymptotic expression for the right eigenvector r_n in the form $r_n = f(u_n)$ and we have replaced $(n + n' + 1)$ with $\max\{(n+1/2)^{t_0/2}, (n'+1/2)^{t_0/2}\}$, which is ensured by the smallness of the parameter t_0 and gives a correction of the order of $O(t_0)$. Fitting the numerical results with an analytical expression (C1), we obtain $c_1 \approx 1.38$ and $c_2 \approx 1.50$ which leads to the answer Eq. (11).

It worth be pointed out that $\lambda_M \approx 1.38/t_0$ lies within the boundary of the Perron–Frobenius inequality,

$$\lambda_M \leqslant \max_n \sum_{n'=0}^{n_{\max}} M_{nn'} \simeq \frac{2}{t_0}. \tag{C3}$$

Next we move on to the case $\mathcal{N} = 0$. Strong spin-orbit coupling corresponds to the matrix $M_{nn'}(\ln n_{\max})$. Again one can find the functional dependence of λ_M on the matrix size $n_{\max}$ with the help of an approximation $\ln(n + n' + 1) \to \ln(\max\{n + 1/2, n' + 1/2\})$. It reveals

$$\lambda_M = \sum_{n'\geqslant 0}^{n_{\max}} \frac{\ln(n_{\max}) - \ln(n'+1)}{n'+1/2}\frac{\Delta_{n'}}{\Delta_0} \simeq \int_{u_\infty}^{u_0} duuf(u) + c_2 \ln n_{\max}. \tag{C4}$$

With the help of Eqs. (39) and (42) and using $\pi^2/(|\gamma_0|t_0) = \ln^2 n_{\max}$, we find the following dimensional fitting,

$$\lambda_M = c_1 \ln^2 n_{\max} + c_2 \ln n_{\max}. \tag{C5}$$

Using the above expression for the fit of numerical data we obtain $c_1 \approx 0.406$, $c_2 \approx 1.57$. Once again, one can check that $c_1 = 0.406$ satisfies the Perron-Frobenius inequality,

$$\lambda_M \leqslant \max_n \sum_{n'=0}^{n_{\max}} M_{nn'}(\ln n_{\max}) \simeq \frac{\ln^2 n_{\max}}{2}. \tag{C6}$$

Appendix D: Local density of states

In the present appendix we discuss details of calculation of the disorder-averaged pair correlation function of the local density of states. Within our approach the mesoscopic fluctuations of the local density of states can be expressed in terms of Q-matrices as follows, see [65, 66],

$$K_2(E, E', \boldsymbol{r}) = \langle\delta\rho(E, \boldsymbol{r})\delta\rho(E', \boldsymbol{r})\rangle = \langle\rho(E, \boldsymbol{r})\rho(E', \boldsymbol{r})\rangle - \langle\rho(E, \boldsymbol{r})\rangle\langle\rho(E', \boldsymbol{r})\rangle = \frac{\nu^2}{32}\,\mathrm{Re}\left[P^{\alpha_1\alpha_2}_{2,irr}(i\varepsilon_1, i\varepsilon_3) - P^{\alpha_1\alpha_2}_{2,irr}(i\varepsilon_1, i\varepsilon_4)\right]. \tag{D1}$$

Here $\alpha_1 \neq \alpha_2$ are some fixed replica indices and analytical continuation, $i\varepsilon_{n_1} \to E + i0$, $i\varepsilon_{n_3} \to E' + i0$, $i\varepsilon_{n_4} \to E' - i0$, is assumed. $P^{\alpha_1\alpha_2}_{2,irr}(i\varepsilon_n, i\varepsilon_m)$ is the irreducible part of bilinear in Q operator,

$$P_2^{\alpha_1\alpha_2} = \langle \mathrm{sp}\, Q^{\alpha_1\alpha_1}_{nn}\, \mathrm{sp}\, Q^{\alpha_2\alpha_2}_{mm} - 2\,\mathrm{sp}\, Q^{\alpha_1\alpha_2}_{nm} Q^{\alpha_2\alpha_1}_{mn}\rangle. \tag{D2}$$

To find mesoscopic fluctuations of the local density of states, we approximate $P_{2,irr}^{\alpha_1\alpha_2}(i\varepsilon_n, i\varepsilon_m)$ as

$$P_{2,irr}^{\alpha_1\alpha_2} \simeq -2\,\mathrm{sp}\langle (R^{-1}WR)_{nm}^{\alpha_1\alpha_2}(R^{-1}WR)_{mn}^{\alpha_2\alpha_1}\rangle. \quad \text{(D3)}$$

Using Eq. (A18), we find the following expression

$$P_2(i\varepsilon, i\varepsilon') = -\frac{32(1+\mathcal{N})}{g}\left[1 - \frac{\varepsilon}{\sqrt{\varepsilon^2+\Delta^2}}\frac{\varepsilon'}{\sqrt{\varepsilon'^2+\Delta^2}}\right] \times \int \frac{d^2\boldsymbol{q}}{(2\pi)^2}\frac{D}{Dq^2+\sqrt{\varepsilon^2+\Delta^2}+\sqrt{\varepsilon'^2+\Delta^2}}, \quad \text{(D4)}$$

that works for all signs of ε and ε'. We point out that this expression is only valid under the assumption (51), when energy dependence of the spectral gap function Δ_ε can be neglected. Then for $K_2(E, E', \boldsymbol{r})$, where $E, E' \gg \Delta$, we find the following lengthy expression,

$$K_2 = \frac{\nu^2(1+\mathcal{N})}{g}\sum_{s=\pm} s\left(1 + \frac{sEE'}{\sqrt{E^2-\Delta^2}\sqrt{E'^2-\Delta^2}}\right) \times \mathrm{Re}\int_q \frac{D}{Dq^2 + i\sqrt{E^2-\Delta^2} - is\sqrt{E'^2-\Delta^2}}. \quad \text{(D5)}$$

Clearly, when $E = E'$, we obtain Eq. (52).

We proceed to mesoscopic fluctuations of the local density of states at different energies $E \neq E'$. First of all, let us note that when energies E and E' are close a pair correlation function $K_2(E, E', \boldsymbol{r})$ differs only slightly from the one on coinciding energies, $K_2(E, E, \boldsymbol{r})$. Therefore the case of energies separated far away from one another is of the interest. Assume that $E' = E + \omega$, where ω is large in comparison to E. Then, expanding the (D5) in a small argument $E/\omega \ll 1$ and performing the integration with respect to momentum $\boldsymbol{q}$ we obtain Eq. (55).

[1] A. A. Abrikosov and L. P. Gor'kov, Sov. Phys. JETP **8**, 1090 (1959).
[2] A. A. Abrikosov and L. P. Gor'kov, Sov. Phys. JETP **9**, 220 (1959).
[3] P. W. Anderson, J. Phys. Chem. Solids **11**, 26 (1959).
[4] P.W. Anderson, Phys. Rev. **109**, 1492 (1958).
[5] L. N. Bulaevskii and M. V. Sadovskii, JETP Lett. **39**, 640 (1984).
[6] M. Ma and P. A. Lee, Phys. Rev. B **32**, 5658 (1985).
[7] A. Kapitulnik and G. Kotliar, Phys. Rev. Lett. **54**, 473 (1985).
[8] G. Kotliar and A. Kapitulnik, Phys. Rev. B **33**, 3146 (1986).
[9] S. Maekawa and H. Fukuyama, J. Phys. Soc. Jpn. **51**, 1380 (1982).
[10] H. Takagi and Y. Kuroda, Solid State Comm. **41**, 643 (1982).
[11] S. Maekawa, H. Ebisawa, and H. Fukuyama, J. Phys. Soc. Jpn. **53**, 2681 (1984).
[12] P. W. Anderson, K. A. Muttalib, and T. V. Ramakrishnan, Phys. Rev. B **28**, 117 (1983).
[13] L. N. Bulaevskii and M. V. Sadovskii, J. Low Temp. Phys. **59**, 89 (1985).
[14] A. M. Finkel'stein, JETP Lett. **45**, 46 (1987).
[15] A. M. Finkel'stein, Physica B **197**, 636 (1994).
[16] D. B. Haviland, Y. Liu, and A. M. Goldman, Phys. Rev. Lett. **62**, 2180 (1989).
[17] A. M. Goldman and N. Marković, Phys. Today **51**, 39 (1998).
[18] V. F. Gantmakher and V. T. Dolgopolov, Physics-Uspekhi **53**, 1 (2010).
[19] B. Sacépé, M. Feigel'man, T. M. Klapwijk, Nat. Phys. **16**, 734 (2020).
[20] M. V. Feigel'man, L. B. Ioffe, V. E. Kravtsov, and E. A. Yuzbashyan, Phys. Rev. Lett. **98**, 027001 (2007).
[21] M. V. Feigel'man, L. B. Ioffe, V. E. Kravtsov, and E. Cuevas, Ann. Phys. **325**, 1390 (2010).
[22] I. S. Burmistrov, I. V. Gornyi, A. D. Mirlin, Phys. Rev. Lett. **108**, 017002 (2012).
[23] I. S. Burmistrov, I. V. Gornyi, and A. D. Mirlin, Phys. Rev. B **92**, 014506 (2015).
[24] M. N. Gastiasoro and B. M. Andersen, Phys. Rev. B **98**, 184510 (2018).
[25] B. Fan and A. M. García-García, Phys. Rev. B **101**, 104509 (2020).
[26] M. Stosiek, B. Lang, and F. Evers, Phys. Rev. B **101**, 144503 (2020).
[27] K. Zhao, H. Lin, X. Xiao, W. Huang, W. Yao, M. Yan, Y. Xing, Q. Zhang, Z.-X. Li, S. Hoshino, J. Wang, S. Zhou, L. Gu, M. S. Bahramy, H. Yao, N. Nagaosa, Q.-K. Xue, K. T. Law, X. Chen, and S.-H. Ji, Nat. Phys. **15**, 904 (2019).
[28] C. Rubio-Verdú, A. M. García-García, H. Ryu, D.-J. Choi, J. Zaldívar, S. Tang, B. Fan, Z.-X. Shen, S.-K. Mo, J. I. Pascual, and M. M. Ugeda, Nano Lett. **20**, 5111 (2020).
[29] I. S. Burmistrov, I. V. Gornyi, and A. D. Mirlin, Ann. Phys. (N.Y.) **435**, 168499 (2021).
[30] M. Stosiek, F. Evers, and I. S. Burmistrov, Phys. Rev. Research **3**, L042016 (2021).
[31] B. Sacépé, C. Chapelier, T. I. Baturina, V. M. Vinokur, M. R. Baklanov, and M. Sanquer, Phys. Rev. Lett. **101**, 157006 (2008).
[32] B. Sacépé, C. Chapelier, T. I. Baturina, V. M. Vinokur, M. R. Baklanov, and M. Sanquer, Nat. Commun. **1**, 140 (2010).
[33] B. Sacépé, Th. Dubouchet, C. Chapelier, M. Sanquer, M. Ovadia, D. Shahar, M. Feigel'man, and L. Ioffe, Nat. Phys. **7**, 239 (2011).
[34] D. Sherman, B. Gorshunov, S. Poran, N. Trivedi, E. Farber, M. Dressel, and A. Frydman, Phys. Rev. B **89**, 035149 (2014).
[35] M. Mondal, A. Kamlapure, M. Chand, G. Saraswat, S. Kumar, J. Jesudasan, L. Benfatto, V. Tripathi, and P. Raychaudhuri, Phys. Rev. Lett. **106**, 047001 (2011).
[36] Y. Noat, V. Cherkez, C. Brun, T. Cren, C. Carbillet, F. Debontridder, K. Ilin, M. Siegel, A. Semenov, H.-W. Hübers, and D. Roditchev, Phys. Rev. B **88**, 014503

(2013).
[37] I. S. Burmistrov, I. V. Gornyi, and A. D. Mirlin, Phys. Rev. B **93**, 205432 (2016).
[38] C. Brun, T. Cren, V. Cherkez, F. Debontridder, S. Pons, L. B Ioffe, B. L. Altshuler, D. Fokin, M. C. Tringides, S. Bozhko, and D. Roditchev, Nat. Phys. bf 10, 444 (2014).
[39] M. Kim, Y. Kozuka, C. Bell, Y. Hikita, and H. Y. Hwang, Phys. Rev. B **86**, 085121 (2012).
[40] K. Ueno, T. Nojima, S. Yonezawa, M. Kawasaki, Y. Iwasa, and Y. Maeno, Phys. Rev. B **89**, 020508(R) (2014).
[41] A. D. Caviglia, S. Gariglio, N. Reyren, D. Jaccard, T. Schneider, M. Gabay, S. Thiel, G. Hammerl, J. Mannhart, and J.-M. Triscone, Nature **456**, 624 (2008).
[42] J. A. Sulpizio, S. Ilani, P. Irvin, and J. Levy, Annu. Rev. Mater. Res. **44**, 117 (2014).
[43] J. T. Ye, Y. J. Zhang, R. Akashi, M. S. Bahramy, R. Arita, and Y. Iwasa, Science **338**, 1193 (2012).
[44] J. T. Ye, Y. J. Zhang, M. Yoshida, Y. Saito, and Y. Iwasa, J. Supercond. Nov. Magn. **27**, 981 (2014).
[45] K. Taniguchi, A. Matsumoto, H. Shimotani, and H. Takagi, Appl. Phys. Lett. 101, 042603 (2012).
[46] K. D. Usadel, Phys. Rev. Lett. **25**, 507 (1970).
[47] M. A. Skvortsov and M. V. Feigel'man, Phys. Rev. Lett. **95**, 057002 (2005).
[48] M. V. Feigel'man and M. A. Skvortsov, Phys. Rev. Lett. **109**, 147002 (2012).
[49] P. A. Lee, J. Non-Cryst. Solids, bf 35, 21 (1980).
[50] T. P. Devereaux and D. Belitz, Phys. Rev. B **44**, 4587 (1991)
[51] W. Brenig, M.-Ch. Chang, E. Abrahams, and P. Wölfle Phys. Rev. B **31**, 7001 (1985).
[52] Y. L. Loh, M. Randeria, N. Trivedi, Ch.-Ch. Chang, and R. Scalettar, Phys. Rev. X **6**, 021029 (2016).
[53] M. Yu. Kagan, E. A. Mazur, JETP **159**, 696 (2021).
[54] A. Abanov, A. V. Chubukov, Phys. Rev. B **102**, 024524 (2020).
[55] Y. Wu, A. Abanov, Y. Wang, A. V. Chubukov, Phys. Rev. B **102**, 024525 (2020).
[56] Y.-M. Wu, A. Abanov, A. V. Chubukov, Phys. Rev. B **102**, 094516 (2020).
[57] Y.-M. Wu, Sh.-Sh. Zhang, A. Abanov, A. V. Chubukov, Phys. Rev. B **103**, 024522 (2021).
[58] Y.-M. Wu, Sh.-Sh. Zhang, A. Abanov, A. V. Chubukov, Phys. Rev. B **103**, 184508 (2021).
[59] Y.-M. Wu, Sh.-Sh. Zhang, A. Abanov, A. V. Chubukov, Phys. Rev. B **104**, 144509 (2021).
[60] P. A. Nosov, I. S. Burmistrov, and S. Raghu, Phys. Rev. Lett. **125**, 256604 (2020).
[61] T. Ch. Wu, Y. Liao, M. S. Foster, arXiv:2206.01762.
[62] E. J. König, A. Levchenko, I. V. Protopopov, I. V. Gornyi, I. S. Burmistrov, and A. D. Mirlin, Phys. Rev. B **92**, 214503 (2015).
[63] E. J. König, I. V. Protopopov, A. Levchenko, I. V. Gornyi, and A. D. Mirlin, Phys. Rev. B **104**, 100507 (2021).
[64] M. R. Beasley, J. E. Mooij, and T. P. Orlando, Phys. Rev. Lett. **42**, 1165 (1979).
[65] I. S. Burmistrov, I. V. Gornyi, and A. D. Mirlin, Phys. Rev. Lett. **111**, 066601 (2013).
[66] I. S. Burmistrov, I. V. Gornyi, and A. D. Mirlin, Phys. Rev. B **91**, 085427 (2015).
[67] A. M. Finkel'stein, *Electron Liquid in Disordered Conductors*, vol. 14 of Soviet Scientific Reviews, ed. by I.M. Khalatnikov, Harwood Academic Publishers, London, (1990).
[68] D. Belitz and T. R. Kirkpatrick, Rev. Mod. Phys. **66**, 261 (1994).
[69] I. S. Burmistrov, JETP, **129**, 669 (2019).